# Climate dynamics on global scale: resilience, hysteresis and attribution of change

Klaus Fraedrich [†], Isabella Bordi [‡] and Xiuhua Zhu [*]

[†] Max Planck Institute of Meteorology, Hamburg, Germany
[‡] University of Rome, La Sapienza, Rome, Italy
[*] University of Hamburg, Hamburg, Germany

**Abstract** The dynamics of a zero- and one-dimensional Energy Balance Model (EBM) of the Earth's climate are subjected to a systematic analysis of the response to changes of the greenhouse effect in terms of atmospheric opacity (effective emissivity), which is related to $CO_2$ concentration. (*i*) Experiments with abrupt $CO_2$-decrease (opacity increase) from the actual value are performed with the one-dimensional EBM, which reveal the following results: There is a critical opacity threshold beyond which the model ends up at a modern snowball Earth. It occurs within a few percentage changes around this threshold because the model strongly depends on the relationship among atmospheric temperature and the sudden ice-albedo feedback activation. Two different time scales characterize the temperature decline; the first almost linear part appears to be related to the change of the opacity and the corresponding sharp increase of the planetary albedo; the second part is mainly controlled by the rapid change of the planetary albedo towards its higher value (ice-albedo feedback). Return from snowball Earth requires a large $CO_2$ concentration as only the ice-albedo feedback is effective while the water vapor feedback is ineffective at low temperatures. Introducing the ice margin as an EBM-variable, hemispheric asymmetry can be identified for different polar albedos while keeping the meridional heat transports. (*ii*) Experiments with transient opacity changes reveal three kinds of hysteresis cycles when introducing cyclic changes: static, dynamic and memory hysteresis. Hysteresis loops are attained for a cyclic change of the greenhouse forcing between the extreme conditions (near bifurcation points) of maximum (almost all outgoing infrared radiation is trapped by the atmosphere) and minimum greenhouse effect (when almost all the infrared radiation is emitted to space). Static hysteresis loops are attained for vanishing heat capacity while dynamic hysteresis shows delay due to the ocean's heat capacity. For cyclic change far from bifurcation points, the model climate depends only on the history

of the radiative forcing thus displaying a hysteresis cycle that is neither static nor dynamical (it does not include bifurcation points nor shows a cyclic steady state), but is related to the memory response of the model determined by the heat capacity (ocean mixed-layer depth).

## 1 Introduction

Common methods of climate model analysis are sensitivity experiments to determine the response to small variations of the external forcing, supposed the system is in a steady state. But such analyses would be misleading when the system has a few steady states. In fact, a small change in the forcing (for example around a $CO_2$ threshold) could lead to a dramatic change in the steady state so that the analysis would not be able to capture the complexity of the system's responses. Therefore, in this contribution to the fluid dynamics of climate we like to extend the traditional sensitivity studies of the climate system analyzing the problem of no return to a fixed forcing and provide a systematic evaluation of two types of forcing change, abrupt and cyclic.

The aim of this chapter[1] is to present – in a comprehensive way – results and novel interpretations of climate dynamics on global scale, that is on resilience, hysteresis and attribution of change; we are focusing on the present day snowball Earth tipping point as it is obtained by changes of greenhouse gas forcing (as described by Bordi et al., 2012, 2013; Fraedrich, 2012). First, the global climate system is introduced as an energy balance model (EBM, Section 2). Here it should be noted that, when long time scales are analyzed, its chaotic nature is averaged out (Held et al., 2010) and only residuals emerge. In this case, a simple model of the surface energy budget can account for most of the responses. Secondly, two characteristic response experiments are conducted and evaluated, both of which affect the greenhouse feedback of the climate system (Section 3); that is, the responses to abrupt and to transient-cyclic changes of the greenhouse forcing. A systematic analysis of the dynamical system reveals three classes of hysteresis: static, dynamic and memory hysteresis. The loop of the latter can be interpreted as a novel phenomenon associated with a dynamic interpretation of resilience, when the system is not affected by tipping points.

[1] A summary of our recent research

## 2 The global climate in a box: Energy Balance Model

To demonstrate climate modeling strategies, a minimum model is introduced first to provide settings for climate analyses. It is based on a poor man's radiation scheme leading to the greenhouse climate system which, when in equilibrium, plays a similar role in climate dynamics as geostrophy and hydrostasy do in geophysical fluid flow. First, the dominant radiative fluxes contributing to the climate are defined in terms of a simple two-stream method, which is reduced to an atmosphere interacting with the land/ocean surface by radiative fluxes only; that is, sensible and latent heat fluxes are not explicitly considered. Parameterization of the atmosphere by statistically deduced feedbacks leads to the statistic-dynamical model version, which is extended to include feedbacks, transient hystereses, and meridional exchanges (and it can be subjected to stability, sensitivity, and stochastic analyses) in order to characterize climate variability.

### 2.1 Dynamical core

Coupling fast atmospheric dynamics with a slow land/ocean, requires a special modeling strategy to explicitly resolve the dynamics of the slow system. A common approach is to parameterize the influence of the fast compartment, which leads to the *statistic-dynamical* climate model with feedbacks incorporating the statistical effects of the fast system. A similar strategy is employed for Global Circulation Models (GCMs) when parameterizing fast and small-scale processes of the boundary layer or cloud ensembles (after suitable space/time-averaging).

**Radiative scheme:** A simple two-stream radiation scheme is introduced with an atmospheric (subscript $A$) and land/ocean or surface (no subscript) layer associated with the respective heat capacities $C_A$ and $C$. Long-wave or terrestrial radiative fluxes are described by the Stefan-Boltzmann law $\sigma T^4$ with $\sigma = 5.67\ 10^{-8}$ $\mathrm{Wm^{-2}K^{-4}}$. The long-wave upward flux from a black body surface, $\sigma T^4$, is absorbed in the upper layer (absorption coefficient $\alpha$), while the long-wave downward radiation is totally absorbed by the surface. The incoming short-wave or solar radiation, $S_0 = 340$ $\mathrm{Wm^{-2}}$, passes a completely transparent atmosphere; it is absorbed at the surface from where a remaining part is reflected to space, $R \downarrow = S_0(1-a)$, with the (planetary) albedo or whiteness $a$. Absorption of solar radiation in the atmosphere would require an additive term contributing to the radiative heating. This leads to a minimum energy balance model of a greenhouse climate with a black body land/ocean surface and without solar absorption

in the atmosphere:

$$\begin{aligned} &\textit{Atmosphere} && C_A(T_A)_t = 0 + \alpha\sigma T^4 - 2\alpha\sigma {T_A}^4 \\ &\textit{Land/Ocean} && CT_t = S_0(1-a) - \sigma T^4 + \alpha\sigma {T_A}^4 \end{aligned}$$

The subscript $t$ attached to the temperatures of the atmosphere and the surface, $T_A$ and $T$, denotes the time derivative. At equilibrium ($C$, $C_A = 0$) the incoming solar radiation balances the long-wave outgoing radiation. First, the atmosphere is considered leaving the land/ocean fixed to provide the boundary conditions ($C = 0$). Its dynamics is relatively fast due to the small heat-capacity, $C_A = c_p(\Delta p/g)$, compared to the ocean heat capacity, $C = 7$ Wm$^{-2}$ K$^{-1}$ year, estimated for a depth of 50 m. The incoming solar radiation $S_0$, planetary albedo $a$, and emissivity $\alpha$, lead to a stable equilibrium with $R_o = R\downarrow = R\uparrow$. The global surface temperature $T = T_A\sqrt[4]{2} \simeq 288$ K satisfies $S_0(1-a) = \sigma T^4(1-\frac{1}{2}\alpha)$, and exceeds the atmosphere's by about 20%. This characterizes the greenhouse effect and corresponds to a vertical temperature difference between surface and atmosphere of $T - T_A \simeq 40$ K. Note that atmospheric temperature, $T_A \simeq 250$ K, to which all initial conditions converge, corresponds to the observed temperature vertically averaged over the atmospheric mass $2\Delta p$, ${T_A}^* = (2\Delta p)^{-1}\int T_A dp$, which is close to the observed mid-troposphere temperature near 500 hPa. Linear stability, $(\delta T_A)_t = -\delta T_A/\tau_A$, of the equilibrium solution is determined by Newtonian cooling with the radiative time scale, $\tau_A = \frac{1}{4}C_A T_A/[\alpha S_0(1-a)]$ of 1 to 2 months.

**Dynamical core:** A suitable Ansatz for the parameterization is a diagnostic atmosphere, $C_A = 0$, which reacts "instantaneously" on changes of the slow system and feeds back to it by the Stefan-Boltzmann effect. This defines the dynamical core of the statistic-dynamical energy balance model (EBM) with effective emissivity (opacity) $\epsilon = (1-b)$ and $b = \frac{1}{2}\alpha$.

$$\textit{Dynamical core} \qquad CT_t = S_0(1-a) - \epsilon\sigma T^4 \tag{1}$$

The knowledge of $T$ at climate steady state ($C = 0$) will allow estimating the atmospheric opacity $\epsilon$ by knowing $S_0$ and $a$. For the present climate $a = 0.3$ and $T = 288$ K so that $\epsilon = 0.61$. For a snowball Earth, instead, we assume $a = 0.7$ and $T = 211$ K which provides a steady solution for $\epsilon = 0.9$. The difference in infrared emission is about 130 Wm$^{-2}$. By instantaneously decreasing $CO_2$ to 20 ppm, we increase the long-wave emission of the atmosphere by just 15 Wm$^{-2}$. Thus, to reach a snowball Earth requires other greenhouse gases, namely the water vapor and its temperature related feedback (see Bordi et al., 2012, and Section 2.2).

### 2.2 Feedbacks and parameterizations

Outgoing and incoming radiation $R\uparrow = \epsilon\sigma T^4$ and $R\downarrow = S_0(1-a)$ include feedback processes affecting the atmospheric emissivity (infrared opacity) $\epsilon$ and surface albedo $a$. They need to be included in the dynamical core describing the statistical (long-term) effects of fast variables on slower ones. Regression-type linear feedbacks are most commonly used in climate modeling modifying the greenhouse climate by its temperature dependent albedo and opacity:

*Ice-albedo effect*: This positive feedback links surface albedo ($0 < a < 1$) and surface temperature.
Temperature-albedo: *temperature drop* $\rightarrow$ *more snow* $\rightarrow$ *higher albedo*
Albedo-temperature: *less SW-radiation absorbed* $\rightarrow$ *further temp. drop*

Various formulations have been employed: The simplest formulations are (i) a quadratic form $a = a_2 - b_2T^2$, (ii) a hyperbolic tangent function of $T$ ranging from $a = 0.3$ to $0.7$, $a = 0.5 - 0.2\tanh\frac{(-20-T)}{10}$, and (iii) a step function interval for the temperature (with $T$ in degree Celsius) with $a = 0.3$ for $T > -10°$C and $a = 0.7$ for $T < -10°$C, which may also describe the limits of the hyperbolic tangent function.

*Greenhouse effect*: This positive feedback associates effective emissivity ($0 < \epsilon < 1$) with the surface temperature, and thus with the atmospheric moisture content as a prominent greenhouse gas.
Temperature-moisture: *temp. rise* $\rightarrow$ *more evaporation* $\rightarrow$ *more vapor*
Moisture-temperature: *more IR radiation from sky* $\rightarrow$ *further temp. rise*

Various formulations are being employed: (i) A positive greenhouse-water vapor feedback, $\epsilon = 1 - b = \epsilon(T)$, which is related to the surface temperature, has been suggested from clear sky radiation measurements in the tropics, $b = c_2 + d_2T^2$. (ii) Considering $CO_2$-emittance only, similar parameterizations are being used based on logarithmic relationships. For example $c_2 = 0.0235\ln(CO_2)$ with $CO_2$ concentration in parts per million by volume (ppm); or assigning a reference value of $C_0 = 280$ ppm, $c_2 = 0.1 + 0.007\ln(CO_2/C_0)$ (Singer et al., 2014); and the $CO_2$-forced heating relation for GCMs, $5.35\ln(CO_2/C_0)$ with a reference $C_0 = 360$ ppm, which has been discussed in IPCC. That is, by decreasing $CO_2$ to 20 ppm (keeping the temperature fixed), the long-wave emission is decreased by merely 15 $Wm^{-2}$.

**Classical applications – resilience, tipping points and attribution:** Employing the quadratic parameterizations of both ice-albedo and greenhouse feedbacks, the EBM introduced here reveals a gradient system (Fig. 1) which has originally been used to demonstrate resilience and catastrophes or tipping points in a zero-dimensional climate system (see Fraedrich, 1979, and Fig. 1): Resilience due to changes in the state variables and in external parameters (forcing) can be measured by suitable integration of the gradient system (or its potential) along the $T$-trajectory from repellor to climate mean at fixed forcing (Fig. 1a) or in parameter space from climate mean to relevant tipping point (Fig. 1b), respectively. Recently this model has been linked with a set of regional socio-economic subsystems to provide a global change analysis incorporating econometric measures of change attribution and to understand the complexity of domestic and international interactions under the global change perspective (see Singer et al., 2014), after adapting the model's performance to past climates and future climate scenarios.

### 2.3 From zero to one dimension

First, we simplify the outgoing long-wave flux parameterization by the first two terms of the binomial expansion of $T^4$ around the reference temperature of 273 K with $T$ in degree Celsius

$$CT_t = S_0(1-a) - \epsilon(A + BT) \tag{2}$$

The coefficients $A = 315$ Wm$^{-2}$, $B = 4.6$ Wm$^{-2}$ °C$^{-1}$ are estimated for an effective emissivity (opacity) $\epsilon = 1$. Anomalies about the reference temperature, $(\delta T)_t = -{\tau_S}^{-1}\delta T$, show its internal stability to which all initial conditions converge. The (negative) eigenvalue represents the slow relaxation time scale $\tau_S = \frac{1}{4}CT/[S_0(1-a)] \simeq 10$ to 20 months $\gg \tau_A$. To include ice margins and meridional transports latitudinal dependence needs to be incorporated; for example, the position of the ice line, cannot be accounted for by the 0-dimensional EBM. However, a surface energy budget that takes this feature into account needs to include meridional heat fluxes $F(T)$ by a simple parameterization (Lindzen, 1990):

$$CT_t = S_0(1-a) - \epsilon(A + BT) + F(T) \tag{3}$$

with $F(T) = k(T^* - T)$, where $T^*$ and $k$ are the global mean surface temperature and the heat-flux coefficient, respectively. For $S_0$ we use the annual average latitudinal dependence (see Bordi et al., 2012, loc. cit.):

$$S_0 = \frac{1}{4}1367(1 - \frac{1}{2}0.477(3x^2 - 1))$$

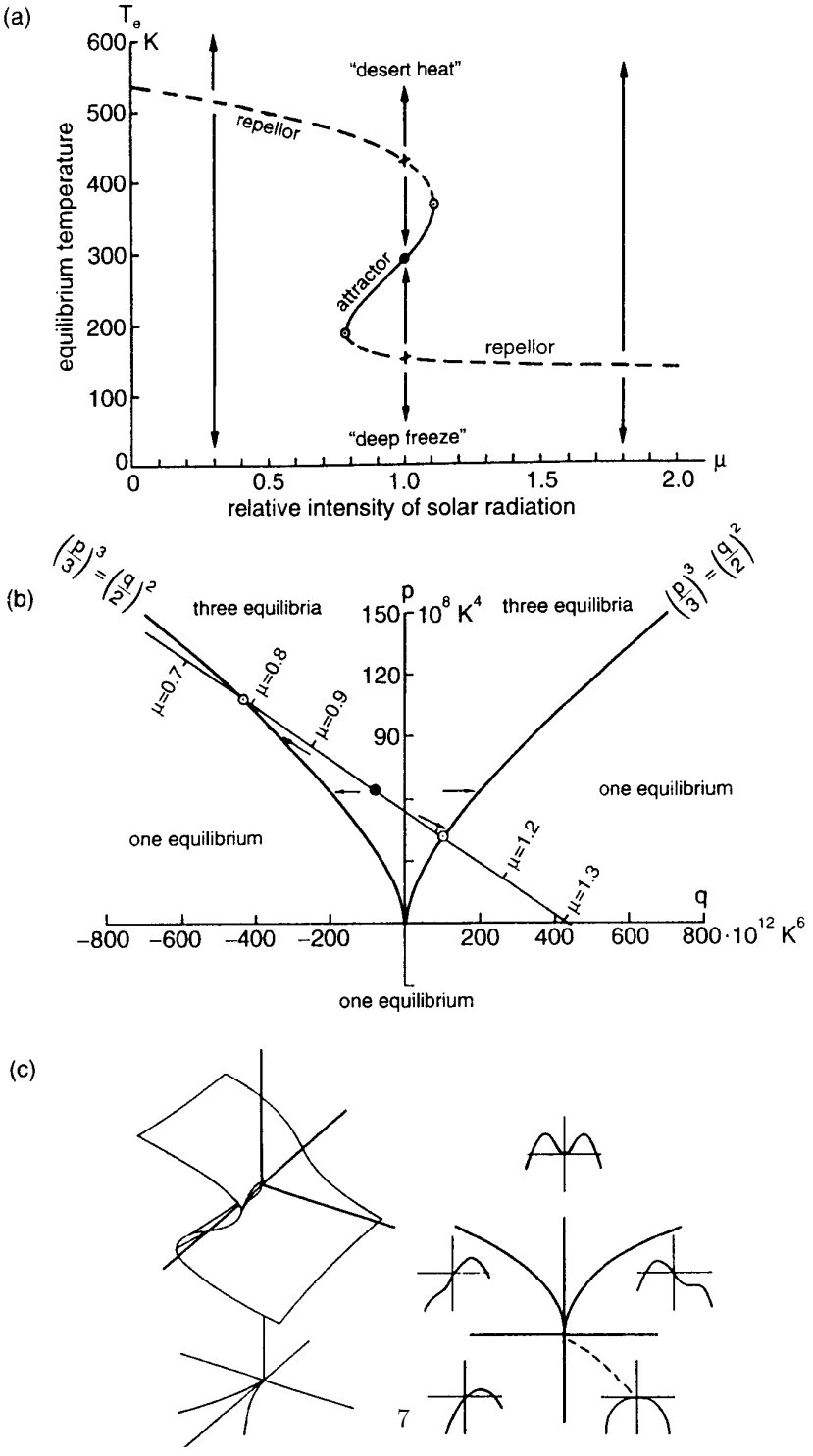


**Figure 1.** Equilibria of a zero-dimensional EBM climate model (gradient system) with ice albedo and greenhouse feedback: (a) state space spanned by the equilibrium surface temperature versus the changing relative solar radiation, (b) bifurcation diagram spanned by generalized (p,q)-axes comprising all external parameters, and (c) schematic presentation of the potential of a gradient system in the generalized parameter space (see Fraedrich, 1979).

where $x = \sin(\phi)$ with $\phi$ being the latitude. Now, with the ice margin temperature $T(X) = -10°\mathrm{C}$ at latitude $X$, the exchange coefficient $k = 2.2\ \mathrm{Wm}^{-2}\ °\mathrm{C}^{-1}$, and the opacity $\epsilon = 0.61$ (for present climate conditions) we obtain $X = 0.95$. To obtain the global mean surface temperature the planetary albedo at the ice margin, $a(X) = (a_1 + a_2)/2$, is required satisfying (in a simple format) the ice-albedo feedback by the step function Ansatz with $a_1 = 0.3$ and $a_2 = 0.62$ below and above the ice margin, respectively. The value of $a_2$ has been chosen to be the averaged surface ice albedo in the Northern Hemisphere (NH) for a snowball Earth state (Bordi et al., 2012, taken from PlaSim simulations). This leads to the global mean surface temperature:

$$T^* = \int_0^1 (S_0(1 - a(x))/\epsilon B - A/B)dx$$

Summarizing, this EBM box model setting provides a toy-modeling approach for dynamical systems diagnostics of abrupt and cyclic changes, expanding the classical tipping point and stochastic analyses.

## 3 Dynamics of hysteresis and resilience: abrupt and cyclic changes

The dynamical model core (Eq. 1) with its suite of parameterizations (Eqs. 2 and 3) will be employed to uncover details of tipping point dynamics which have not been discussed in the classical analyses (in the seventies) and the more recent rediscovery about thirty years later. As tipping point we select the transition to modern snowball Earth by changing the greenhouse feedback induced by the terrestrial radiation contribution to the Earth's energy balance. In contrast to the commonly analyzed effect of changing solar radiation input (due to the Milankovich cycles) we change the $CO_2$-related terrestrial radiation affecting the dynamics induced by ice-albedo and water-vapor greenhouse feedbacks. *Abrupt changes* are analyzed first (Bordi et al., 2012): (i) What are the time scales before reaching what appears to be a bifurcation or tipping point towards modern snowball Earth? (ii) How functions the back-transition from the modern snowball Earth, when the CO2 concentration is set to very large values keeping the solar constant at present value? (iii) How are radiative perturbations related to the latitude of the ice margin? (iv) And are there hemispheric asymmetries induced by radiative effects, that is cooling one hemisphere more than the other? *Cyclic changes* are analyzed next (Bordi et al., 2013) to account for hysteresis effects, which range from (i) static via (ii) dynamic to (iii) memory hysteresis.

### 3.1 Abrupt change dynamics

The setting to analyze the dynamics induced by abrupt changes is the dynamical core of the 0-dimensional EBM (Eq. 1) amended by the ice-albedo and the greenhouse feedback parameterizations and the extension to a 1-dimensional system introduced in the previous section on model development.

**Towards snowball Earth:** The dynamical core (Fig. 2a, Eq. 1) combined with the hyperbolic-tangent ice-albedo feedback function of $T$ (ranging from $a = 0.3$ to 0.7) is integrated with increasing the initial value from present day $\epsilon = 0.61$ up to 0.9 at a given time rate to mimic the long wave radiative effect of the $CO_2$. This corresponds to a reduction towards 20 ppm where the transition to snowball Earth occurs. The transition from low albedo values to the higher one at 0.7 occurs at the threshold $T = -20°C$. The time-dependent solution shows that the surface temperature (after adjusting to perturbation) decreases (i) almost linearly from its initial value of about 15°C toward about $-10°C$ and then (ii) when it crosses the threshold of the major albedo change at $-20°C$ (at $a = 0.7$), it quickly decreases to about $-60°C$. This is the equilibrium temperature if all parameters are kept constant from then on. That is, two different time scales characterize the temperature decline: (i) The first part appears to be related to the change of the opacity $\epsilon$ and the corresponding sharp increase of the planetary albedo. (ii) The second part is mainly controlled by the rapid change of the planetary albedo toward its higher value (ice-albedo feedback). Note that this simple EBM is able to capture the same features of the surface temperature behavior as provided by the GCM PlaSim (see Bordi et al., 2013).

**Return from snowball Earth:** The dynamical core reveals a range of external parameters $\epsilon$ (or $S_0$) characterized by the co-existence of two stable solutions: snowball and temperate Earth. This range depends on (i) the threshold temperature at which the planetary albedo changes and (ii) the sharpness of this transition (Fig. 2b). This is shown by the temperature steady states when varying $\epsilon$ back and forth within the opacity $\epsilon$-interval 0.2 - 0.9: The planetary albedo step function ($a = 0.3$ and 0.7, black line) shows that the transition between these boundary values occurs at $T = -10°C$. The planetary albedo hyperbolic tangent function (blue and red lines) centered at $T = -10°C$ and $T = -20°C$, respectively. This shows that if the system is in a snowball state, and if we increase a greenhouse gas such as $CO_2$, we might escape from this state provided that the associated radiative forcing $\epsilon$ reaches the threshold value identified by the lower branch

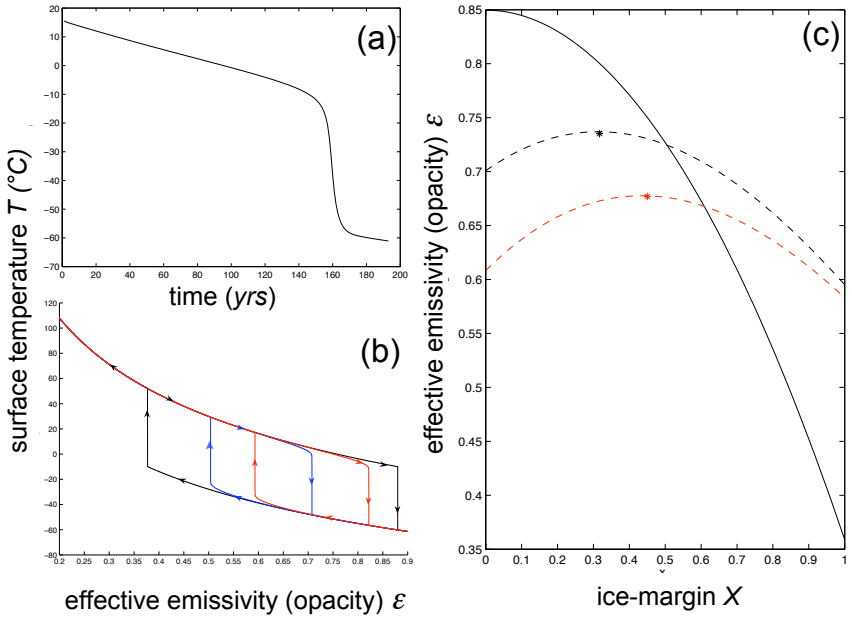


**Figure 2.** EBM analysis: (a) Time evolution of the surface temperature $T$ obtained by integrating the 0-dimensional energy balance model (Eq. 2) for the opacity $\epsilon$ varying linearly from 0.61 to 0.9. The parameters settings are listed in the text. (b) Steady solutions (Eq. 2) for the surface temperature $T$ as a function of $\epsilon$ varying back and forth in the interval 0.2-0.9. The shape of the planetary albedo is specified in the text. Arrows denote the direction of variation of $\epsilon$. Units are dimensionless and degree Celsius for $\epsilon$ and $T$, respectively. (c) Radiative forcing $\epsilon$ as a function of the ice margin $X$ (solution of Eq. 4) for $\beta = 0$ and $a_2 = 0.62$ (solid black line), $\beta > 0$ and $a_2 = 0.62$ (dashed black line), $\beta > 0$ and $a_2 = 0.7$ (solid red line). Asterisks denote the maximum of the curves for $\beta > 0$. Units are dimensionless (see Bordi et al., 2013).

of the hysteresis curves. Moreover, it is predicted that the new state will be a great deal warmer than what is expected because we must add also the water vapor effect that dominates once the evaporation has been re-established and it involves the insulating nature of ice. Also, the rate of approach to the two steady state branches is just a consequence of the sharpness of the albedo change associated with the ice-albedo feedback activation or deactivation. In particular, Fig. 2b (red line) shows the transition from snowball to ice-free Earth to occur for $\epsilon = 0.59$ in case of setting the $T$-bound to $-20$°C. This value of the greenhouse forcing must be provided by adding only $CO_2$, since the water vapor effect is excluded due to lack of evaporation. This explains why the large value of $CO_2$ concentration is needed for the transition back from the ice-covered state.

**Radiation – ice margin relation:** The latitudinal dependence of the ice line can only be considered by a 1-dimensional EBM (Fig. 2c, Eq. 3). Normally, we expect that the ice margin moves towards the equator ($X = 0$) as the radiative forcing $\epsilon$ increases and vice-versa. The presence of heat transports should destabilize this unique relationship (ice cap instability) by introducing a critical ice margin $X^*$ so that for any $X < X^*$ there is only the snowball solution. Thus, to study the behavior of $\epsilon$ as a function of $X$, all the other parameters are fixed. It turns out that by evaluating Eq. 3 at $X$ (with $C = 0$ or steady state condition), the opacity $\epsilon$ must satisfy the following diagnostic equation:

$$\epsilon^2 \Lambda_1 + \epsilon^2 \Lambda_2 + \Lambda_3 = 0 \tag{4}$$

where the coefficients $\Lambda_i$ ($i = 1, 2, 3$) are functions of the parameters evaluated at a given $X$. In Fig. 2c (black lines) the solutions as a function of $X$ are shown in case of $\beta = 0$ (solid line) and $\beta \neq 0$ (dashed line). Note that for a given $X$ there are two real solutions; the negative one must be excluded since $\epsilon > 0$. Note also that in case of no heat transports, for each $\epsilon$-value in the interval 0.35-0.85 within the bifurcation points (roughly the same range is identified in Fig. 2, black line) there is a unique value of $X$. When heat transports are active, they cool the equatorial regions and warm the polar ones. This implies that lower values of $\epsilon$ are sufficient to allow the ice to advance towards the tropics, while the opposite holds at high latitudes. Moreover, it appears that a critical $X$ exists for which the solution is in a snowball state (the ice forms also in the tropics). In our case, $X^* = 0.32$ (or 18.7°N) which corresponds to the maximum values of $\epsilon$. This is the critical latitude beyond which the ice is expand to the equator. Moreover, it appears that for $\epsilon$ between 0.7 and 0.74 (maximum value) two ice margins satisfy the diagnostic equation. Since the heat fluxes introduce

a critical ice margin so that the ice can form also in the tropics, they are a key parameter for the transition to snowball state and vice versa, and a characteristic feature of the dynamics of this snowball Earth tipping point.

**Hemispheric asymmetry:** Since in the SH the surface albedo of the ice is expected to be higher than in the NH (as supported by GCM simulations when the ice-covered state is reached), let us consider the solution of the diagnostic equation with the same heat transports but $a_2 = 0.7$ (red dashed line in Fig. 2c). In this case, the range of variability of the radiative forcing associated with the ice margin is reduced and, most importantly, the critical ice margin is changed to $X^c = 0.45$, which corresponds to about 26.7°N. This means that the snowball Earth solution is reached more rapidly for a higher value of $a_2$ because the critical latitude of the ice margin is moved poleward. This explains asymmetries between NH and SH, which is particularly evident when ozone is removed. In concluding, the origin of the asymmetric response between the NH and SH lies in the different ice albedo of the two hemispheres.

In summarizing, sudden decrease of atmospheric trace gases that interact with thermal radiation shows the following effects: If there are bifurcation points, the dynamics depends crucially on the exact amount of the gas concentrations as long as their effect on water vapor is significant. There appears to exist a $CO_2$ threshold leading to a modern snowball Earth. The response of the thermal field has a great degree of simplicity; that is, when long time scales are analyzed with the chaotic behavior being averaged out only residuals occur (Held et al., 2010). Thus, a simple energy balance model may account for many aspects of climate dynamics.

### 3.2 Cyclic change dynamics – hysteresis and resilience

The response of a zero-dimensional energy balance model (Eq. 2, linearized dynamical core) is studied. It includes the ice-albedo feedback by the step-function approach and the greenhouse effect expressed by effective surface emissivity, $\epsilon = (1 - b)$; the outgoing infrared radiation changes between the extreme conditions of maximum and minimum greenhouse effect, $b \in [1 > b_1 > b_2]$, representing cyclic changes of $CO_2$-concentration, which contrasts the commonly studied Milankovic cycles affecting the incoming solar radiation cycles. The following cycle is restricted not to include the bifurcation points:

$\beta(t) = \beta_{01} - bt$ for $t$ from $(n-1)\tau$ and $n\tau$ for $n = 1, 3, 5, ...$
$\beta(t) = \beta_{02} + b(t-\tau)$ for $t$ from $(m-1)\tau$ and $m\tau$ for $m = 2, 4, 6, ...$

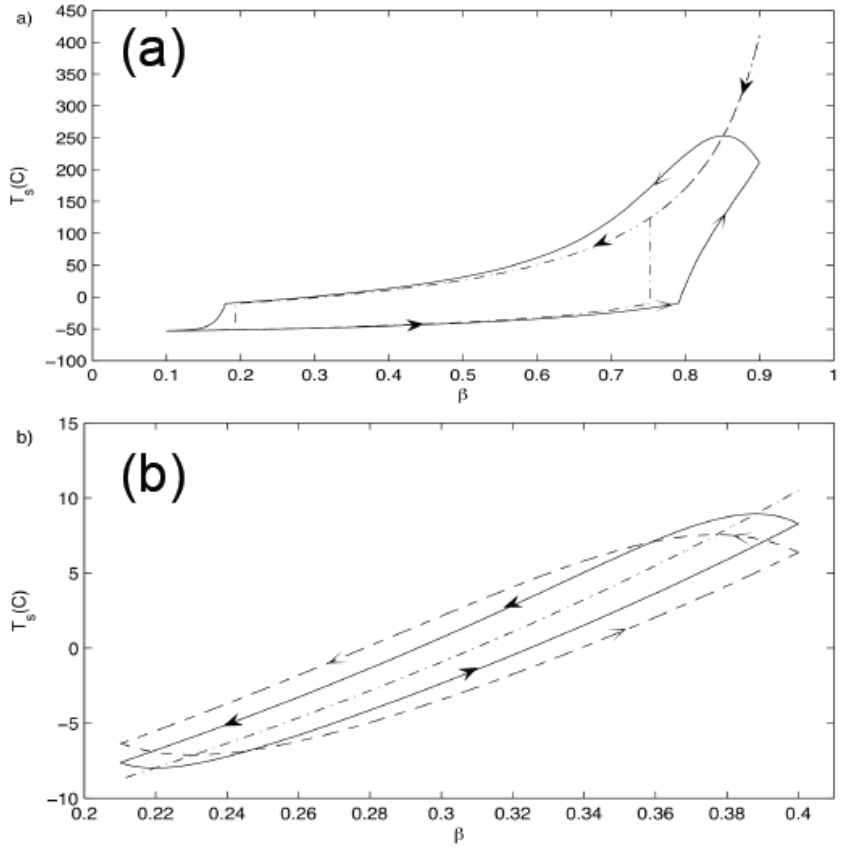


**Figure 3.** EBM solutions in $(\beta, T)$-plane: (a) Static hysteresis loop (dash-dotted) for $C = 0$ and $\beta$ varying statically back and forth in the interval [0.9, 0.1], and dynamical hysteresis loop (solid line) for $C = 50$ Wm$^{-2}$ K$^{-1}$ year and $\beta$ varying in the same interval at the rate $b = 0.001$ year$^{-1}$. (b) Locus of steady states (dash-dotted) for $C = 0$ and $\beta$ varying statically in the interval [0.4, 0.21], and memory hysteresis loops for $C = 50$ Wm$^{-2}$K$^{-1}$year (solid), $C = 100$ Wm$^{-2}$ K$^{-1}$year (dashed) and $\beta$ varying in the same interval at the rate $b = 0.001$ year$^{-1}$. Units are dimensionless and in degree Celsius for $\beta$ and $T$ (see Bordi et al., 2013).

with the half-cycle time $\tau = (\beta_1 - \beta_2)/b$, and the boundary conditions $\beta_1 = \beta((n-1)\tau) = 0.9$ and $\beta_2 = \beta((m-1)\tau) = 0.1$ determine $\beta_{01}$ and $\beta_{02}$. The selected boundary values represent the extreme conditions of maximum greenhouse effect (almost all outgoing infrared radiation is trapped by the atmosphere) and of minimum greenhouse effect (when almost all the infrared radiation is emitted to space). Two "cyclic" EBM experiments are performed, that is one with and one without including the bifurcation points into the cycle.

**Cycle with bifurcation points:** So far, two types of hysteresis experiments are being distinguished.
*Static hysteresis*: If the heat capacity $C$ is set to zero and $\beta$ varies extremely slowly (adiabatically) back and forth within in the selected $\beta$-interval, then a static hysteresis loop appears (Fig. 3a, dash-dotted). This corresponds to the conventional time slice approach performed by global climate model experiments analyzing climate change under varying radiative forcing conditions.
*Dynamic hysteresis*: For $C = 50$ $\mathrm{Wm^2K^{-1}yr}$ and $\beta$ varying back and forth in the same $\beta$-interval at the rate $b = 0.001$ $\mathrm{yr}^1$, a dynamical hysteresis loop emerges (Fig. 3a, solid curve). Within the $\beta$-range the values of radiative forcing, which lead to the transition from ice-free to ice-covered Earth state and vice versa, can be easily estimated from the upper and lower branches of the hysteresis cycles. Note that by construction, such transitions occur when there is a change in the albedo $a$, i.e. the surface temperature crosses the threshold of $-10°$C. Note that the dynamical hysteresis shows different transition points compared to the static hysteresis.

**Cycle without bifurcation points:** There is a dynamical hysteresis without bifurcation. To illustrate this case, consider $\beta$ within [0.4, 0.21] so that the system is linear with $T > -10°$C and $a = 0.35$. Note that $\beta = 0.4$ is an estimation of the greenhouse parameter for present climate ($a = 0.35$ and $T = 15°$C); the value of $\beta = 0.21$, instead, has been estimated from Fig. 3a as lower bound of $\beta$ before transition to the ice-covered Earth state. For $C = 0$, the solution of the EBM will follow the continuous set of steady states determined by the $\beta$-value at a given time without static hysteresis. For $C \neq 0$, instead, the solutions will depart from the steady states because of the delayed response of the system induced by the heat content (l.h.s. of EBM). This departure is expected to be positive when $\beta$ decreases and negative when $\beta$ increases. Since the end points are fixed, the two branches will join there, so that the full cycle follows a closed curve in

the $(\beta, T)$-plane.

**Memory hysteresis and resilience:** Define $\beta$ as input, the linear core as transducer, and $T$ as observation, then the solution is a dynamical hysteresis loop but without a static counterpart. Therefore, such a loop cannot be attributed as static or dynamical hysteresis (as in Goldsztein et al., 1997), because it does not represent the locus of the steady states and it does not include the bifurcation points. Therefore, we coin it memory hysteresis which is due to a kind of memory effect. That is, the system responds on a longer time scale compared to the forcing change by a time delay of adjustment to the time-dependent forcing variation. Given a time rate of change of radiative forcing, the source of this memory effect lies in the heat capacity $C$ whose magnitude controls the width of the hysteresis loop. For this case entropy is not a well-defined quantity, as the area enclosed in the loop will not equal the entropy production. Instead, the area is a measure of the resilience (and of the memory) to the time-dependent change of the forcing. The EBM trajectories are displayed as hysteresis loops in a $(\beta, T)$-space for a given time rate b and two values of heat capacity $C$ (Fig. 3b). The dash-dotted curve is the locus of the model steady states ($C = 0$), while the time-dependent solutions for decreasing (increasing) $\beta$ are shown for large (dashed) and small (full) heat capacities. Three features are noted: First, for different greenhouse gas parameters we obtain the same temperature. Second, when the model switches from decreasing to increasing $\beta$ (or vice versa) the model response lags the forcing so that the surface temperature will continue to increase (or decrease) despite the fact that the forcing is already decreasing (or increasing). Third, an increasing heat capacity $C$ enhances the effect of the system's memory broadening the memory hysteresis loop and thus enhancing resilience.

**Recalcitrant response:** The lagged memory response is not associated with the recalcitrant or slow response (see Held et al., 2010): Two heat capacities characterize the dynamics, a shallow ocean layer responding rapidly to the atmosphere, and a deeper ocean which are responsible for the fast and slow components observed in the GCM response, though it has a similar effect. The slow component of the global warming refers to a climate model response towards equilibrium by an instantaneous return to the preindustrial radiative forcing. The problem of no "return" to a fixed forcing which our systematic hysteresis analyses are related to, is different, as the forcing is cyclically changed at a given time rate and transient (not steady) solutions are followed. Moreover, this EBM has a single time scale, which is determined by the heat capacity $C$ (consistent with GCM-PlaSim simu-

lations). For any rate of $CO_2$ change, the relaxation towards equilibrium for $CO_2 = 20$ ppm is characterized by a single time scale dictated by the depth of the slab ocean. Thus, the slow component has a different origin in the two cases: In the study by Held et al. (2010) it is related to the slow adjustment of the system towards equilibrium to a sudden reduction of the radiative forcing, while in the present study it is due to the delay of the system in adjusting to the time-dependent forcing variations. The area enclosed by the loop may be a relevant parameter to be considered when greenhouse gases are projected into different future values; climate, in fact, may be trapped by loops like these.

## 4 Conclusions

A climate system with bifurcation points as been introduced has an energy balance model associated with ice-albedo and greenhouse-temperature feedbacks. Its dynamics has been analyzed by a set of experiments to characterize the response to abrupt and transient-cyclic greenhouse forcings. The novel features revealed in an EBM environment have also been observed in global climate model simulations following the same experimental design (as described by Bordi et al., 2012, 2013; Fraedrich, 2012). This substantiates the observation that, when long time scales are analyzed, the chaotic nature of the climate system is averaged out (Held et al., 2010) and only residuals emerge. The results presented in this lecture note are in parts a linear combination of a set papers (Bordi et al., 2012, 2013; Fraedrich, 2012). The aim is twofold: First, to extend climate system analyses to transient forcing and present the methods and results in the energy balance model framework. Secondly, to note that the design of comprehensive global climate model experiments, in particular when employing transient forcings, should be preceded by a thorough analysis of a simpler surrogate climate system of the type of energy balance models, which are subjected to the same suite of conditions.

## Acknowledgements

We thank Professor Alfonso Sutera for decade-long collaboration, continuing discussions, inspirations and exchanges.

## Bibliography

Bordi, I., K. Fraedrich, A. Sutera, X. Zhu, *Transient response to well-mixed greenhouse gas changes*, Theor. Appl. Climatol., **108**, 245-252,

doi:10.1007/s00704-011-0580-z, 2012.

Bordi, I., K. Fraedrich, A. Sutera, X. Zhu, *On the effect of decreasing $CO_2$ concentrations in the atmosphere*, Clim. Dyn., **40**, 651-662, doi:10.1007/s00382-012-1581-z, 2013.

Fraedrich, K., *Catastrophes and resilience of a zero-dimensional climate system with ice-albedo and greenhouse feedback*, Q. J. Roy. Meteorol. Soc., **105**, 147-167, 1979.

Fraedrich, K., *A suite of user-friendly global climate models: Hysteresis experiments*, Eur. Phys. J. Plus, **127**, 127:53, doi: 10.1140/epjp/i2012-12053-7, 2012.

Goldsztein, G. H., F. Broner, S. H. Strogatz, *Dynamical hysteresis without static hysteresis: scaling laws and asymptotic expansions*, SIAM J. Appl. Math., **57**, 1163-1187, 1997.

Held, I. M., M. Winton, K. Takahashi, T. Delworth, F. Zeng, G. K. Vallis, *Probing the fast and slow components of global warming Transient response to well-mixed greenhouse gas changes by returning abruptly to preindustrial forcing*, J. Climate, **23**, 2418-2427, doi:10.1175/2009JCLI3466.1, 2010.

Lindzen, R. S., *Dynamics in Atmospheric Physics*, Cambridge, University Press, New York, 1990.

Singer, C., T. Milligan, T. S. Gopi Rethinaraj, *How China's options will determine global warming*, Challenges, **5**, 1-25, doi:10.3390/challe5010001, 2014.